

# Articles

## An MC-SCF Study of the Thermal and Photochemical Cycloaddition of Dewar Benzene

Ian J. Palmer,<sup>†</sup> Massimo Olivucci,<sup>†</sup> Fernando Bernardi,<sup>\*,‡</sup> and Michael A. Robb<sup>\*,†</sup>

*Dipartimento di Chimica "G.Ciamician" dell'Universita di Bologna, Via Selmi 2, 40126 Bologna, Italy, and Department of Chemistry, King's College, London, Strand, London WC2R 2LS, U.K.*

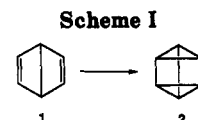
Received June 10, 1992

The thermal and photochemical transformation of Dewar benzene (1) to prismane (2) is studied using MC-SCF methods with a 4-31G basis. The thermal synchronous  $[2_s + 2_s]$  process does not exist because the "antiaromatic" transition state has two imaginary frequencies. Rather, the preferred thermal mechanism corresponds to a cisoid quasi one-step asynchronous process (transition state, diradical minimum, transition state separated by less than 2 kcal mol<sup>-1</sup>). A pathway leading to a transoid diradical intermediate does exist but has an energy that is so high that it is of no chemical significance. This diradical is a nonreactive diradical since the radical centers cannot close via rotation about the cross bond. However this path is photochemically accessible. The "classical"  $[2_s + 2_s]$  structure on the excited-state surface that has a geometry similar to the "anti-aromatic" transition state on the ground state is not an avoided crossing minimum but rather a transition state. The central feature of the photochemical mechanism is a conical intersection between ground- and excited-state surfaces that lies between Dewar benzene and prismane. The system undergoes a fully efficient return to the ground state via this conical intersection and can proceed either to prismane or to Dewar benzene. The factors that control the topology of the ground- and excited-state potential surfaces have been analyzed using a VB model. The exchange energy shows clearly the origin of the conical intersection. The constraint of the cagelike framework of the molecule manifests itself in the Coulomb energy. This fact may explain why only the adiabatic photochemical reaction is observed in 1,4-Dewar naphthalene where the  $\sigma$ -bond framework cannot distort (without breaking the aromaticity of the second ring) to the conical intersection geometry observed in the  $[2 + 2]$  photochemical transformation of Dewar benzene to prismane.

### Introduction

The thermal stability of nonaromatic benzene isomers (such as prismane, Dewar benzene, and benzvalene) is an example of the powerful restrictions imposed by the principle of conservation of orbital symmetry. In contrast, photochemical transformations of the various isomers of benzene are readily accomplished (see the general refs 1 or 2). The photochemical mechanisms involve nonadiabatic reaction pathways. Thus, the excited state of one isomer correlates directly with the ground state of another. However, very little is known about the details of the possible reaction pathways that must lead from the excited state directly to products. To our knowledge, the only case that has been studied theoretically in any detail is the reaction of the  $S_1$  state of benzene. Here it has been suggested<sup>3</sup> that the  $S_1$  state of benzene "crosses" with the  $S_0$  state of prefulvene along a reaction path that connects benzene and prefulvene. Clearly, an understanding of the detailed mechanism of such transformations is essential to the rationalization of the mechanisms of intramolecular photochemical valence transformations which are useful synthetic reactions. The objective of this paper is an understanding of the thermal and photochemical mechanism of one of the simplest such transformations Dewar benzene (1) to prismane (2).

This information may help to rationalize the important field of intramolecular  $[2 + 2]$  cycloadditions in general.



This transformation between 1 and 2 is formally a thermally forbidden  $[2_s + 2_s]$  cycloaddition. However, Turro<sup>4</sup> has shown that a significant yield of prismane is produced via  $S_1$  by direct photolysis of Dewar benzene (although benzene is the major product). Similarly, direct excitation of prismane yields minor amounts of Dewar benzene (with benzene as the major product). Turro has demonstrated experimentally that the appearance of benzene in both reactions is a result of secondary singlet-triplet absorption of Dewar benzene itself which initiates a quantum chain reaction that results in the production of benzene. No adiabatic ring opening reactions of 1 or 2 to produce benzene are observed in singlet states. Thus, both photochemical reactions are experimentally observed to be nonadiabatic processes. In contrast, 1,4-Dewar naphthalene and Dewar anthracene<sup>5</sup> undergo only an adiabatic photochemical ring opening reaction to excited naphthalene and anthracene. As a result of theoretical calculations,<sup>6</sup> we now have some insight into the thermal and

(1) Turro, N. J. *Modern Molecular Photochemistry*; Benjamin Cummings: Menlo Park, CA, 1978; pp 499-503.

(2) Bryce-Smith, D.; Gilbert, A. *Rearrangements in Ground and Excited States*; de Mayo, P., Ed., Academic Press: 1980, pp 349-379. Bryce-Smith, D.; Gilbert, A. *Tetrahedron* 1976, 32, 1309-1326.

(3) Kato, S. *J. Chem. Phys.* 1988, 88, 3045-3056.

(4) Turro, N. J.; Ramamurthy, V.; Katz, T. J. *Nouv. J. Chim.* 1977, 1, 363-365.

(5) Carr, R. V.; Kim, B.; McVey, J. K.; Yang, N. C.; Gerhartz, W.; Michl, J. *Chem. Phys. Lett.* 1976, 39, 57-60.

(6) (a) Bernardi, F.; Bottoni, A.; Robb, M. A.; Schlegel, H. B.; Tonachini, G. *J. Am. Chem. Soc.* 1985, 107, 2260-2264. (b) Bernardi, F.; Olivucci, M.; Robb, M. A. *Acc. Chem. Res.* 1990, 23, 405-412. (c) Bernardi, F.; De, S.; Olivucci, M.; Robb, M. A. *J. Am. Chem. Soc.* 1990, 112, 1737-1744.

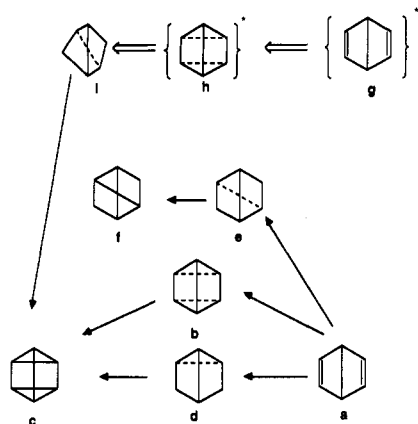


**Figure 1.** Mechanistic pathways for the thermal (a-b-c, a-d-c, a-e-f) and photochemical (g-h-i-c) transformation of Dewar benzene.

photochemical mechanism of the prototypical [2 + 2] cycloaddition of two ethylene molecules. However, photochemical intramolecular [2 + 2] cycloadditions are much more important synthetically, yet unstudied from a theoretical point of view. The Dewar benzene to prismane transformation is well-documented experimentally and thus provides a good example for theoretical study.

For the Dewar benzene to prismane transformation, one can postulate several ground- and excited-state reaction pathways as illustrated in Figure 1. In fact, as we shall presently discuss, all these mechanistic pathways actually exist although the nature of the potential energy surface and the importance of the various reaction pathways is influenced by the constraint of the  $\sigma$  framework. For example, one might expect that a diradical intermediate for the "formal" two-step asynchronous reaction (f) would be rather high in energy. Further, it is a pathway leading to a nonreactive diradical with no further possibility of getting to prismane due to the constraint imposed by the Dewar benzene cage (i.e., the system cannot rotate about the "cross bond" to close the diradical).

While the theoretical study of the mechanism of the thermal transformation from Dewar benzene to prismane involves the characterization of intermediates and transition structures in the usual way, the central feature of the photochemical pathway that must be studied is the nature of the potential surface "funnel"<sup>7</sup> where a nonadiabatic radiationless transition takes place and the system returns from the excited state to the ground state. The funnel mechanism is based upon the model of Oosterhoff.<sup>7a</sup> In this model, the excited state branch of the reaction path terminates in an "avoided crossing minimum" on the excited state and then undergoes radiationless decay to the ground state. The efficiency of this decay is determined by the gap between ground and excited state, and unless this gap is very small the process will be inefficient<sup>7b</sup> and other events (e.g., fluorescence) may happen on a shorter time scale. After radiationless decay via the "funnel", the course of the photochemical reaction becomes determined by the nature of the ground-state surface itself. In early computations Gerhartz et al.<sup>8</sup> have shown that the "funnel"

can be a conical intersection where a real surface crossing occurs. In more recent work<sup>9</sup> we have been able to show that such conical intersections may be a common feature of photochemical reactions. (Theoretical discussion of such conical sections can be found in reference<sup>10</sup>). The most important aspect from a mechanistic point of view is that at a conical intersection the return to the ground-state surface is fully efficient. Recent dynamics computations<sup>10l</sup> have shown that the decay from excited-state surface to ground state via a conical intersection occurs in less than one vibrational period. Thus, the existence of an energetically accessible conical intersection as the reaction funnel can provide the central feature for a nonadiabatic photochemical reaction if it lies in a chemically interesting region of the excited-state potential energy surface.

### Methodological Details

Since the ground-state [ $2_s + 2_s$ ] cycloaddition of Dewar benzene is a forbidden reaction and there is the possibility of diradical intermediates SCF (restricted or unrestricted) cannot give a correct zeroth order description of the surface. Accordingly, we have used the implementation of MC-SCF method,<sup>11</sup> a complete active space (CAS) form, distributed in GAUSSIAN 90.<sup>12</sup> In MC-SCF the orbitals for an excited state can be optimized using higher roots of the CI eigenvalue problem. In this problem the choice of the active orbitals is completely unambiguous: the four Dewar benzene  $\pi$  orbitals and the  $\sigma$  and  $\sigma^*$  orbitals of the bridgehead  $\sigma$  bond. The inclusion of the  $\sigma$  and  $\sigma^*$  orbitals of the bridgehead  $\sigma$  bond will improve the description of the rather stretched C-C bridgehead bond in Dewar benzene. Note that this active space will not give a completely symmetric structure for prismane itself since three of the C-C  $\sigma$  bonds will be in the active space and the remaining six will not. Unless indicated otherwise the 4-31G basis has been used for all computations.

While the location of minima and transition states is readily accomplished using standard methods, the location of the "funnel" from the excited-state surface to the ground-state surface is not so straightforward and we now give some discussion of the point. We begin with a definition of a conical intersection: *Two surfaces, even with the same symmetry, intersect in an  $n - 2$  dimensional hyperline as the energy is plotted against the  $n$  nuclear coordinates.* (See for example the discussion in the book of Salem<sup>7c</sup>). At a conical intersection, one can distinguish two directions, say  $\mathbf{x}_1$  and  $\mathbf{x}_2$ , such that if one were to plot the energy in the subspace of these two geometric variables (combinations of the bond lengths angles, etc.) the potential energy would have the form of a double cone in the region of the degeneracy. In the remaining  $n - 2$  directions, the energies of ground and excited states are equal. Movement in the plane  $\mathbf{x}_1$  and  $\mathbf{x}_2$  lifts this degeneracy. The two vectors  $\mathbf{x}_1$  and  $\mathbf{x}_2$  correspond to the nonadiabatic coupling vector  $\langle \psi_1 | \partial \psi_2 / \partial s \rangle$  and the gradient difference vector  $\partial(E_2 - E_1) / \partial s$  where  $s$  is a nuclear displacement vector. The gradient difference vector

(9) (a) Bernardi, F.; Olivucci, M.; Robb, M. A. *J. Am. Chem. Soc.* **1992**, *114*, 5805-5812. (b) Bernardi, F.; Olivucci, M.; Ragazos, I. N.; Robb, M. A. *J. Am. Chem. Soc.* **1992**, *114*, 2752-2754.

(10) (a) Von Neumann, J.; Wigner, E. *Physik. Z.* **1929**, *30*, 467. (b) Teller, E. *J. Phys. Chem.* **1937**, *41*, 109. (c) Herzberg, G.; Longuet-Higgins, H. C. *Trans. Faraday Soc.* **1963**, *35*, 77. (d) Herzberg, G. *The Electronic Spectra of Polyatomic Molecules*; Van Nostrand: Princeton, 1966; p 442. (e) Mead, C. A.; Truhlar, D. G. *J. Chem. Phys.* **1979**, *70*, 2284. (f) Mead, C. A. *Chem. Phys.* **1980**, *49*, 23. (g) Keating, S. P.; Mead, C. A. *J. Chem. Phys.* **1985**, *82*, 5102. (h) Keating, S. P.; Mead, C. A. *J. Chem. Phys.* **1987**, *86*, 2152. (i) Davidson, R. E.; Borden, W. T.; Smith, J. J. *J. Am. Chem. Soc.* **1978**, *100*, 3299. (j) Mead, C. A. The Born-Oppenheimer approximation in molecular quantum mechanics. In Truhlar, D. G., Ed. *Mathematical frontiers in computational chemical physics*; Springer: New York, 1987; Chapter 1, pp 1-17. (k) Blais, N. C.; Truhlar, D. G.; Mead, C. A. *J. Chem. Phys.* **1988**, *89*, 6204. (l) Manthe, U.; Koppel, H. *J. Chem. Phys.* **1990**, *93*, 1658.

(11) Robb, M. A. In *Self-Consistent Field-Theory and Applications*; Carbo, R., Klobukowski, M., Eds.; Elsevier: New York, 1990; p 278.

(12) GAUSSIAN 90. Frisch, M. J.; Head-Gordon, M.; Trucks, G. W.; Foresman, J. B.; Schlegel, H. B.; Raghavachari, K.; Robb, M.; Binkley, J. S.; Gonzalez, C.; Defrees, D. J.; Fox, D. J.; Whiteside, R. A.; Seeger, R. A.; Melius, C. F.; Baker, J.; Martin, R. L.; Kahn, L. R.; Stewart, J. J. P.; Topiol, S.; Pople, J. A. Gaussian, Inc., Pittsburgh PA, 1990.

(7) (a) Van der Lugt, W. T. A. M.; Oosterhoff, L. J. *J. Am. Chem. Soc.* **1969**, *91*, 6042. (b) Gimbert, D.; Segal, G.; Devaquet, A. *J. Am. Chem. Soc.* **1975**, *97*, 6629. (c) Michl, J.; Bonacic-Koutecky, V. *Electronic Aspects of Organic Photochemistry*; Wiley: New York, 1990. (d) Bonacic-Koutecky, V.; Koutecky, J.; Michl, J. *Agnew. Chem., Int. Ed. Engl.* **1987**, *26*, 170-189. (e) Salem, L. *Electrons in Chemical Reactions: First Principles*; Wiley: New York, 1982.

(8) Gerhartz, W.; Poshusta, R. D.; Michl, J. *J. Am. Chem. Soc.* **1977**, *99*, 4263.

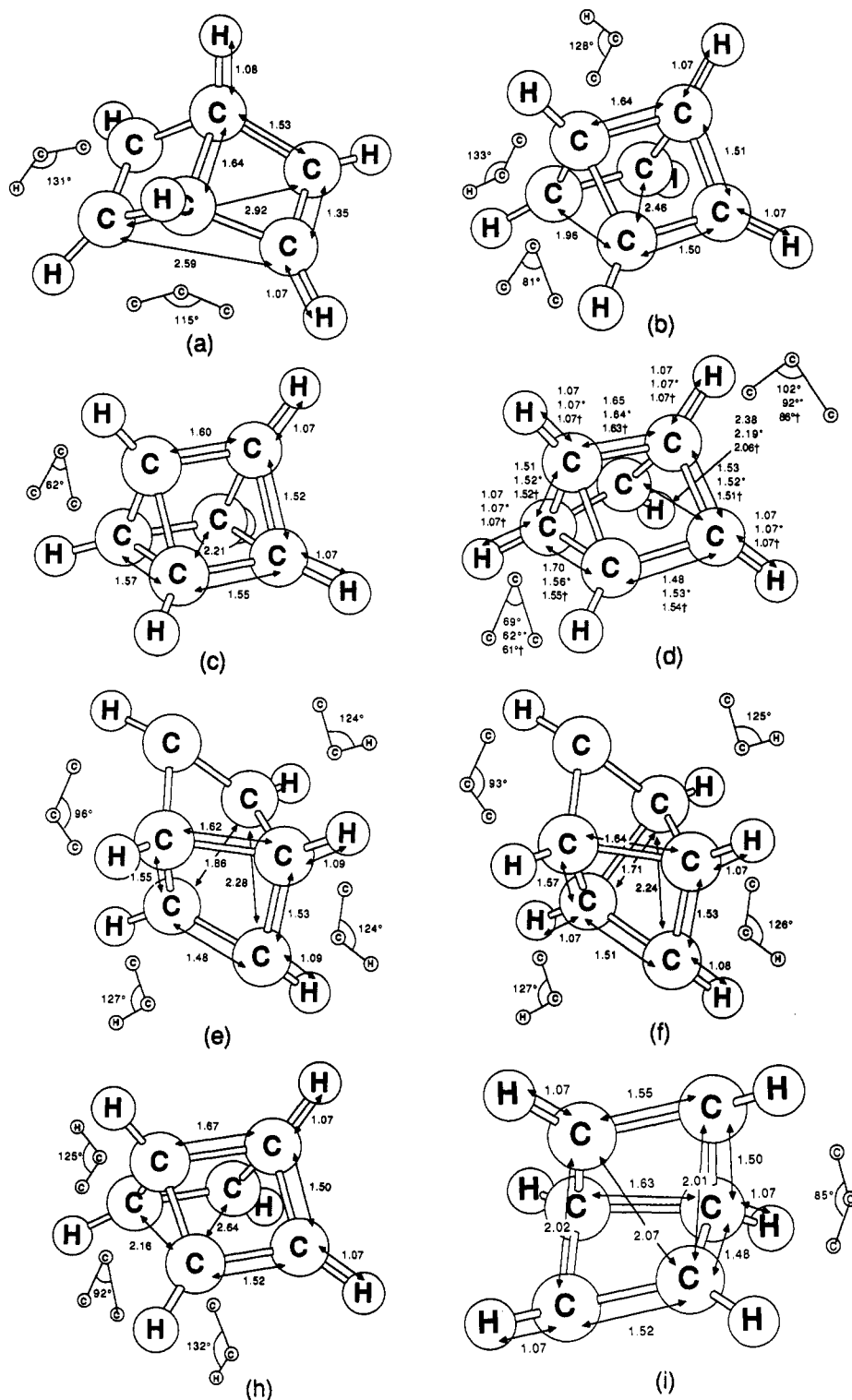


**Figure 2.** Optimized geometries of critical points on the ground- and excited-state potential energy surface for thermal and photochemical cycloaddition of Dewar benzene. Bond distances are in Å and angles in deg. The labels a, b, etc. correspond to the schematic representation in Figure 4. The structure d comprises three geometries: (i) a transition state for the formation of the first bond, (ii) the intervening diradical minimum, and (iii) the transition state for the formation of the second bond. All geometries are optimized at the CAS(6 in 6)/4-31G level with the exception of e which could only be optimized at the STO-3G level.

always "points" to the "bottom" of the cone and the nonadiabatic coupling vector is approximately at 90°.

We are interested in the lowest energy point on this hyperline which corresponds to a well-defined geometry of the system. Thus, in the optimization, the energy is minimized in  $n - 2$  variables while the vectors  $\mathbf{x}_1$  and  $\mathbf{x}_2$  are constraints. The gradient on the excited-state potential energy surface will not be zero at a conical intersection point, since it "looks like" the vertex of an inverted cone. Rather the gradient is only zero in the  $n - 2$  dimensional space orthogonal to  $\mathbf{x}_1$  and  $\mathbf{x}_2$ . This situation is distinguished from a "touching" or "avoided crossing minimum" of two surfaces where

the gradient on the excited state potential energy surface would go to zero. The actual algorithm used in the optimization is similar to that reported in ref 13 and uses state averaged orbitals.

## Results and Discussion

**(i) Structural Results and Energetics.** The structures of the various critical points on the possible mechanistic pathways of Figure 1 are illustrated in Figure 2.

**Table I. Energies of Critical Points on the Prismane Dewar Benzene Potential Energy Surface**

structure	nature	$E_h$	rel energy (kcal mol <sup>-1</sup> )
Dewar benzene <b>a</b>	minimum	-230.3010	0
<b>b</b>	two imaginary frequencies	-230.1477	96
<b>d</b>	(a) transition state	-230.1680	83.4
	(b) diradical minimum	-230.1711	81.5
	(c) transition state	-230.1708	81.7
prismane <b>c</b>	minimum	-230.1966	66
<b>e/f</b>	minimum <sup>a</sup>	-230.1339	105
<b>h</b>	transition state	-230.0801	139
<b>i</b>	conical intersection <sup>b</sup>	-230.0814 ( $E_1$ )	138
		-230.0810 ( $E_2$ )	
Dewar benzene to benzene	transition state	-230.2693	19.9
benzene	minimum	-230.4543	-96.2

<sup>a</sup>Using an STO-3G basis (which overstabilizes diradicaloid geometries) we find both a diradical minimum **f** and the transition structure **3**. At the 4-31G level the surface in this region was very flat and it proved to be impossible to obtain good convergence. Thus, we were able to locate only the minimum **f**. Thus, the geometry of **f** obtained is not completely optimized (a maximum force of 0.008 au and an RMS force of 0.003 au). <sup>b</sup>State averaged MC-SCF calculation.

The corresponding energetic information is given in Table I. We also give the energies for the transition state connecting Dewar benzene and benzene itself for reference. We shall present a "global view" of the surface subsequently.

A note on the accuracy of our calculations is appropriate here. In order to obtain reliable energetics one must perform a computation with a method that includes dynamic correlation in an extended basis including polarization basis functions. Our objective here is less ambitious; we are concerned with the surface topology and structural information. With MC-SCF at the 4-31G level we obtain the correct surface topology (i.e., number and nature of critical points that occur in possible mechanistic pathways). The validity of this assertion has been tested recently on the potential energy surface for the [2 + 2] cycloaddition of two ethylenes. In recent work<sup>14</sup> we have reoptimized the structures obtained in earlier work<sup>6a</sup> using an extended basis. The surface topology remains the same as the 4-31G results. The energetics (barrier heights) obtained at the MC-SCF MP2<sup>15</sup> level were shown to be in acceptable agreement with experimental values. (For example, the computed barrier height for the formation cyclobutane via cycloaddition of two ethylene molecules at the MC-SCF MP2 level is 44.7 kcal mol<sup>-1</sup> as compared with the experimental value of 43 kcal mol<sup>-1</sup>.)

In addition to the above, one must point out that the basis set used and the choice of active space implies that certain parts of the excited state surface cannot be described. Since we do not have diffuse orbitals in the basis we cannot describe ionic/Rydberg states. Thus, we cannot investigate the photophysical part of the reaction following photoexcitation. However, our objective is the investigation of the photochemical part of the surface where bonds are made and broken. There may be barriers that arise in the region of the surface that corresponds to vertical excitation (probably to Rydberg states); however, we cannot study this region accurately without the use of more extended basis sets and an active space that includes diffuse orbitals.

For the ground-state forbidden [ $2_s + 2_s$ ] Dewar benzene to prismane thermal process we see that the synchronous "transition state" **b** has two imaginary frequencies and an asynchronous path **a-d-c** is preferred. The structure **d** actually comprises a shallow minimum and two transition states separated by less than 2 kcal mol<sup>-1</sup>. Thus, this region of the surface is very flat and the reaction path is best described as two-stage asynchronous.

Remarkably a highly asynchronous "formal" two-step process **a-e-f-c** for Dewar benzene to prismane transformation also exists. This process involves a highly strained "cross" diradical intermediate shown in Figure 2f with a "cross" C-C bond length (1.71 Å). However, this pathway is only "formal" since the diradical **f** cannot react (by rotation about the cross bond) to produce **c** via ring closure. This pathway is of very high energy and of no chemical interest in the thermal reaction; however, this region of the surface is accessible in the photochemical reaction and we return to this point subsequently. We were able to characterize the structure **f** only crudely at the 4-31G level because the hessian had near zero eigenvalues (for **f** we have maximum force of 0.008 au and an RMS force of 0.003 au, and we have located **3** only at the STO-3G level). However, accurate geometries and energies are not of any interest for this region.

For the excited-state surface we have characterized two structures; **h** which has a structure similar to the ground-state [ $2_s + 2_s$ ] "transition state" **b** and a conical intersection **i**. The structure **h** has one well-defined negative eigenvalue in the Hessian and one eigenvalue that is very small. As a consequence the geometry is not well defined. The negative direction of curvature corresponds to rhomboidal distortion toward the conical intersection **i** which lies on the line that connects **h** and **f**. In general, all our computations are insensitive to using a four-orbital four-electron CAS-SCF as opposed to a six-orbital six-electron CAS-SCF (the extra orbitals/electrons corresponding to the bridgehead bond). The nature of **h** is an exception because the highly strained geometry stretches the bridgehead C-C bond considerably. For the four-orbital four-electron CAS-SCF this structure is a shallow minimum with one very small Hessian eigenvalue while at the six-orbital six-electron CAS-SCF the structure is a transition state.

The central novel result for the photochemistry is the existence of the conical intersection **i**. Thus, the excited-state molecule returns to the ground state between Dewar benzene and prismane to a point on the ground-state surface that lies above the transition structures **b** or **d**. As discussed previously, the subspace of nuclear motion that corresponds to the double cone is spanned by the gradient difference vector  $\mathbf{x}_2 = \partial(E_2 - E_1)/\partial s$  and the nonadiabatic coupling vector  $\mathbf{x}_1 = \langle \psi_1 | \partial \psi_2 / \partial s \rangle$ . The orientation of these vectors is shown in Figure 3. Notice that these two vectors correspond to (a) a coordinate that involves primarily the distance between the ethylenic fragments and (b) a coordinate that involves the rhomboidal distortion from a rectangular arrangement of the two ethylenic fragments. Depending upon dynamical considerations (i.e., the trajectory being followed as the system passes through the conical intersection) the system will either proceed to prismane or Dewar benzene along a coordinate that is a linear combination of the vectors  $\mathbf{x}_1$  and  $\mathbf{x}_2$  (ie rhomboidal distortion and relative motion of the two ethylenic fragments). Thus, the conical intersection provides a point of rapid return from the excited state to Dewar benzene before rearomatization can take place. Thus, the existence of the conical intersection is compatible with the experi-

(14) Bernardi, F.; Bottoni, A.; Venturini, A.; Robb, M. A. *Chem. Phys. Lett.* 1992, 192, 237.

(15) McDouall, J. J.; Peasley, K.; Robb, M. A. *Chem. Phys. Lett.* 1988, 148, 183.

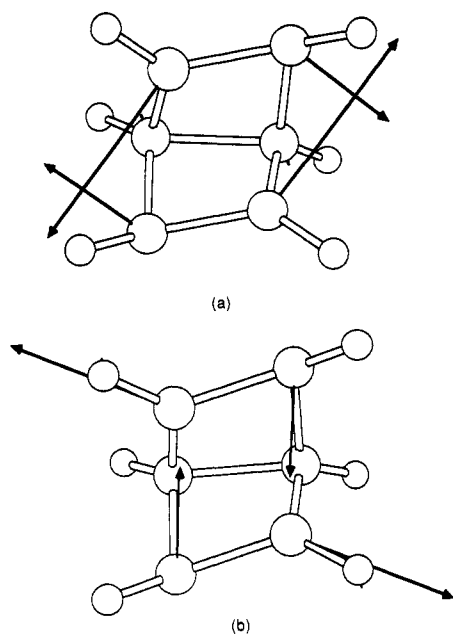


**Figure 3.** The two-dimensional subspace of the conical intersection *i*. (a) The gradient difference vector  $\partial(E_2 - E_1)/\partial s$  and (b) the nonadiabatic coupling vector  $\langle \psi_1 | \partial \psi_2 / \partial s \rangle$ .

mental observations (a) photolysis of Dewar benzene yields prismane and (b) photolysis of prismane yields Dewar benzene (benzene is produced by secondary reaction of Dewar benzene<sup>4</sup>).

(ii) **Global Analysis Using a VB Model.** In addition to the structural and energetic information just discussed, it is useful to consider more qualitative models that can be used to explain and visualize the topology of the potential surface and hence to rationalize other related experimental results. In ref 16 we have discussed how the surface topology can be visualized using a VB model and a qualitative summary of the detailed ab-initio results produced. The essence of the model is the decomposition of the energy into a coulomb contribution  $Q$  and an exchange contribution  $T$

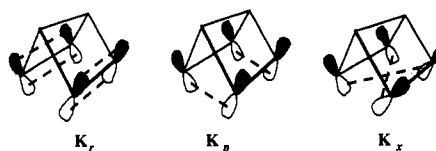
$$E = Q \pm T \quad (1)$$

The Coulomb energy incorporates the steric and electrostatic effects that arise from the  $\sigma$  framework, while the effects of electronic reorganization of the ethylenic  $p^\pi$  orbitals manifest themselves in  $T$ . In ref 16a we have described how the MC-SCF results can be transformed to a VB representation, and a modeling technique has been derived<sup>16b</sup> that uses a combination of VB and molecular mechanics (MM-VB). The energy evaluation in this procedure is so fast that one can generate quite large grids of data that can be used to obtain a global view of interesting regions of the potential energy surface that are easily visualized. In this section we present a global summary of the MC-SCF results in this form.

The exchange energy  $T$  is the representation of the electronic reorganization effects. It is convenient to use a four-electron four-orbital model involving the double bond  $p^\pi$  orbitals of Dewar benzene. In this case  $T$  can be decomposed into two center exchange integrals between the active  $p$  orbitals as

$$T = [(K_P - K_X)(K_R - K_X) + (K_P - K_R)^2]^{1/2} \quad (2)$$

Chart I



The exchange integrals  $K_P$ ,  $K_R$ , and  $K_X$  are sums of two center exchange terms

$$K_R = K_{12} + K_{34} \quad K_P = K_{13} + K_{24} \quad K_X = K_{14} + K_{23} \quad (3)$$

The  $K_{ij}$  are proportional to the corresponding orbital overlaps; thus, we can visualize the  $K_R$ ,  $K_P$ , and  $K_X$  as shown in Chart I. Clearly, by virtue of eq 2, the ground and excited states have a conical intersection when  $T = 0$ , i.e.

$$K_P = K_X, K_R = K_X, K_P = K_R \quad (4)$$

Thus, the *existence* of a conical intersection is controlled by a geometrical distortion required to satisfy eq 4 (i.e., the electronic reorganization of the ethylenic  $p^\pi$  orbitals); however, the energetic accessibility of a conical intersection is controlled by the behavior of  $Q$  (i.e., by the nature of strain effects that arise from the framework). We now illustrate this effect.

As discussed previously, the minimum energy point on the conical intersection is characterized by a molecular structure, and two vectors that correspond to the two constraints. Thus, in order to visualize the conical intersection region, one should plot the energy in the subspace of two geometric variables (combinations of the bond lengths, angles, etc.) that correspond to the nonadiabatic coupling vector and the gradient difference vector. In this subspace, the potential energy should obviously have the form of a double cone in the region of the degeneracy. In Figure 4 we show potential energy diagrams in the space of two geometrical motions (a) the distance between the C=C fragments and (b) a coordinate that corresponds to rhomboidal distortion from a rectangular arrangement of the two C=C fragments suggested by these vectors. In each case the detailed geometries were obtained by parabolic interpolation between the various optimized geometries.

On the left of Figure 4 we show the total energy for ground and excited state while the coulomb  $Q$  and exchange  $T$  are shown on the right. One can observe that the excited-state antiaromatic structure **h** corresponds to a shallow minimum along the pathway for the transformation of Dewar benzene to prismane. There is then a transition state before the conical intersection. (Since we have used four active orbitals to maintain the correspondence between the simple model just discussed, this has the effect of increasing the bridgehead C-C bond stretching potential turning structure **h** into a shallow minimum rather than a transition structure at the six active orbital levels. This artifact is observed in the MC-SCF computations as well but disappears when the bridgehead CC bond is included in the active space. However, this does not affect the more qualitative aspects that we would like to discuss at this point.) The occurrence of the condition on the exchange integral eq 4 is clearly seen as the singularity in the exchange energy  $T$ . The values of the exchange integrals, computed from ab-initio MC-SCF data, are shown in Figure 5 and the condition of eq 4 is clearly met. The  $\sigma$  framework of structures **i** and **f** is very strained. Thus, the coulomb energy  $Q$  (which incorporates the steric effects that arise from the  $\sigma$

(16) (a) Bernardi, F.; Olivucci, M.; McDouall, J. J. W.; Robb, M. A. *J. Chem. Phys.* 1988, 89, 6365. (b) Bernardi, F.; Olivucci, M.; Robb, M. A. *J. Am. Chem. Soc.* 1992, 114, 1606.

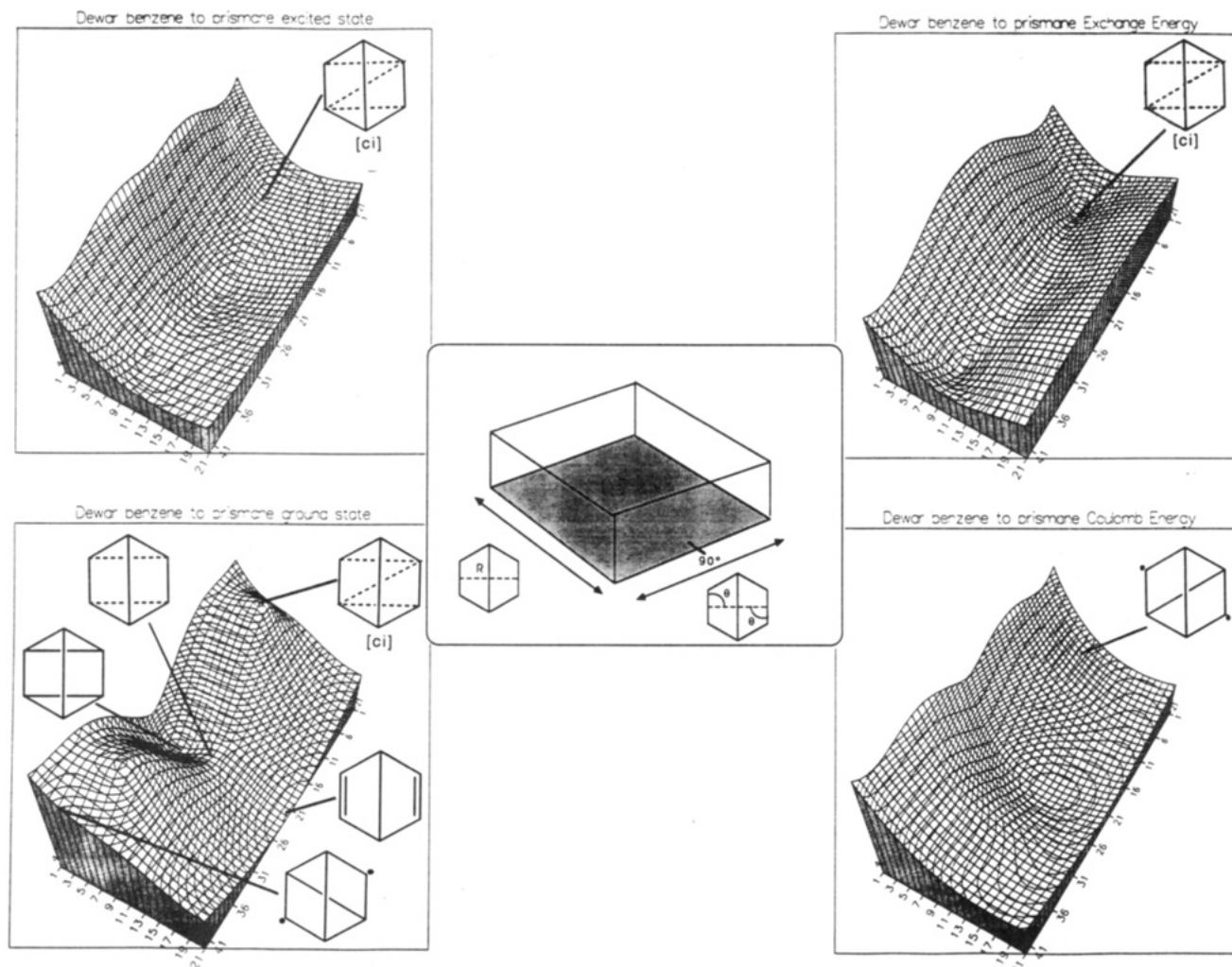


**Figure 4.** Decomposition of the ground- (bottom left) and excited-state (top left) potential energy surfaces into Coulomb (bottom right) and exchange (top right) energies for the thermal and photochemical cycloaddition of Dewar benzene.

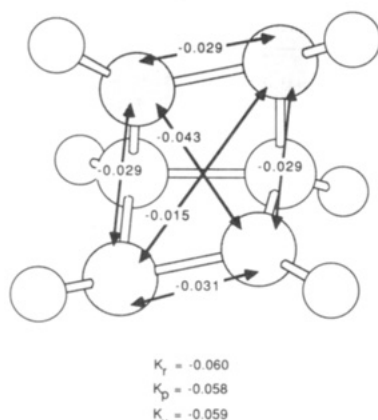


**Figure 5.** Exchange integrals from a CAS (4 in 4)/4-31G effective Hamiltonian computation<sup>16a</sup> at the conical intersection geometry to verify the condition given in eq 4.

framework) for the transformation of Dewar benzene to prismane is strongly repulsive and shows a ridge along the rhomboidal distortion coordinate. As a consequence, the existence of an energetically accessible conical intersection is very delicate for the intramolecular transformation of Dewar benzene to prismane. The occurrence of this ridge in  $Q$  is due to the ring strain induced by rhomboidal distortion. If this ring strain were to be increased, the conical intersection must still exist (since it is controlled by electronic effects); however, it will be moved to higher

energy turning the "anti-aromatic" structure into a deep minimum. In fact, we artificially induce this effect by increasing the bridgehead stretching potential when we use four rather than six orbitals for the active space. This observation is consistent with experiment: only the adiabatic photochemical reaction is observed in 1,4-Dewar naphthalene where the  $\sigma$ -bond framework cannot distort (without breaking the aromaticity of the second ring) to the conical intersection geometry observed in the [2 + 2] photochemical the transformation of Dewar benzene to prismane.

### Conclusions

The distinct features of the ground-state potential energy for the transformation of Dewar benzene to prismane are (a) the thermal pathway for the transformation of Dewar benzene to prismane involving a transoid diradical intermediate has an energy so high that it is of no chemical significance and (b) the cisoid diradical path exists as the preferred pathway. The photochemical conversion of Dewar benzene to prismane occurs via a conical intersection between ground- and excited-state surfaces. The "classical" structure on the excited-state surface that corresponds to the "antiaromatic" transition state on the ground state is not a minimum but rather a transition state that connects two equivalent transoid ground-state minima via two equivalent conical intersections. The system undergoes a fully efficient return to the ground state via this conical intersection and can proceed to either prismane



or Dewar benzene (and to benzene via a secondary process<sup>4</sup>).

The differences between an intermolecular [2 + 2] cycloaddition (the [2 + 2] reaction of two ethylene molecules<sup>6</sup> that we have studied previously) and the intramolecular [2 + 2] cycloaddition of Dewar benzene to prismane merit some brief comment. The differences ought to be capable of rationalization from behavior of the Coulomb energy  $Q$  (i.e., to steric effects that arise from the  $\sigma$  bond framework) since the exchange energy  $T$  must have a similar topology in the two systems. While the coulomb energy  $Q$  in the [2 + 2] cycloaddition of two ethylene molecules is completely flat (see Figure 4 of ref 6b) and plays almost no role in the determination of the topology of the ground- and excited-state potential energy surfaces, as we have seen,  $Q$  plays a crucial role in the mechanism of the transformation of Dewar benzene to prismane. Thus, in contrast to the [2 + 2] cycloaddition of two ethylene molecules, where the lowest energy pathway involves an asynchronous two-step process involving an anti attack, the corresponding thermal pathway for the transformation of Dewar benzene to prismane involving a nonaromatic transoid diradical intermediate is only a "formal" pathway

since the diradical intermediate is unreactive and has an energy so high (because of the constraint of the  $\sigma$  frame) that it is of no chemical significance. Rather, the preferred thermal mechanism for transformation of Dewar benzene to prismane corresponds to a two-stage asynchronous process. In the [2 + 2] cycloaddition of two ethylene molecules the "transition state" on this pathway has two imaginary frequencies; however, the constraint of the  $\sigma$  frame turns one of these negative directions positive in the Dewar benzene to prismane transformation. The electronic factors that control the existence of the conical intersection are present in both systems. However the geometry at the conical intersection is so highly strained (large  $Q$ ) for the transformation of Dewar benzene to prismane that this mechanism may not exist if steric factors are increased consistent with the experimental observation that only the adiabatic photochemical reaction is observed<sup>5</sup> in 1,4-Dewar naphthalene.

**Acknowledgment.** This work was supported by the SERC (U.K.) under grant numbers GR/F 48029, GR/F 46452, and GR/G 03335. I.J.P. is grateful to the SERC for the award of a studentship.

## Photoinduced Reduction of Aldehydes on Titanium Dioxide

Cheryl Joyce-Pruden, Jeffrey K. Pross, and Yuzhuo Li\*

Department of Chemistry, Clarkson University, Potsdam, New York 13699-5810

Received April 6, 1992

Aromatic and aliphatic aldehydes are reduced to their corresponding alcohols using titanium dioxide as a photocatalyst. The reduction proceeds through an electron transfer from the excited state of titanium dioxide to the aldehydes and is followed by a protonation. The electron hole in the valence band of the excited semiconductor causes concomitant oxidation of the alcohol solvent and production of hydrogen. The quantum efficiency for the reduction is directly related to the half-wave potential of the aldehyde, the solvent, the nature of an electron donor, and the presence of a strong acid or base.

Study of light-induced electron-transfer reactions on semiconductors has become one of the most active areas of research in photochemistry. The reactions demonstrate the possibilities of converting solar energy into chemical or electrical energy, providing new synthetic routes, and introducing new ways of photodegradation of industrial wastes.<sup>1</sup> Titanium dioxide is one of the most studied semiconductors due to its ultraviolet-visible absorption band and chemical stability. Irradiation of titanium dioxide promotes one electron from the valence band (VB) to the conduction band (CB). The excited state of  $\text{TiO}_2$  can be expressed as  $\text{TiO}_2(e^-, h^+)$ .<sup>2</sup> The electron in the conduction band is readily available for transference ( $-0.85$  eV vs SCE) while the electron hole in the valence band is open for donation (2.4 eV vs SCE).<sup>3</sup> A reactant that receives the electron from  $\text{TiO}_2$  would be reduced, while a reactant that donates an electron to  $\text{TiO}_2$  would be oxidized. Based on this redox scheme, a variety of organic reactions can be catalyzed by semiconductors. For example, oxidation of protic organic compounds or biomass to produce hydrogen<sup>4</sup> and photodegradation of polychloroaromatic compounds have been explored.<sup>5</sup> Photo-

oxidations of organic compounds such as amines, carboxylic acids, and aromatic olefins<sup>6</sup> on semiconductors also have been fruitfully investigated. However, there are only a few reports on the reduction of organic compounds using a semiconductor as a photocatalyst.<sup>7</sup> Reduction of acet-

(1) (a) Kalyanasundaram, K. in *Energy Resources Through Photochemistry and Catalysis*; Grätzel, M., Ed.; Academic Press: New York, 1983; pp 217-260. (b) Pelizzetti, E.; Barbeni, M.; Pramauro, E.; Erbs, W.; Borgarello, E.; Jamieson, M. A.; Serpone, N. *Quimica Nova* 1985, 288. (c) Halmann, M.; Zuckerman, K. In *Homogeneous and Heterogeneous Photocatalysis*; Pelizzetti, E., Serpone, N., Eds.; D. Reidel: Dordrecht, 1988; pp 521-532.

(2) (a) Wrighton, M. S. *Photochemistry, Chem. Eng. News*, Sept 3, 1979; pp 29-47. (b) Fox, M. A. *Nouv. J. Chim.* 1987, 11, 129.

(3) Kanno, T.; Oguchi, T.; Sakuragi, H.; Tokumaru, T. *Tetrahedron Lett.* 1980, 21, 467.

(4) (a) Borgarello, E.; Pelizzetti, E. *Chim. Ind.* 1983, 65, 474. (b) Teratani, S.; Nakamichi, J.; Taya, K.; and Tanaka, K. *Bull. Chem. Soc. Jpn.* 1982, 55, 1688. (c) Sakata, T.; Kawai, T. In *Energy Resources Through Photochemistry and Catalysis*; Grätzel, M., Ed.; Academic Press: New York, 1983; pp 331-358. (d) Noudek, L.; Sedlacek, J. *J. Catal.* 1975, 40, 34.

(5) (a) Matthews, R. W. *Wat. Res.* 1990, 24, 653. (b) Frank, S. N.; Bard, A. J. *J. Am. Chem. Soc.* 1977, 99, 7729. (c) Pelizzetti, E.; Serpone, N.; Borgarello, E. In *Photocatalysis and Environment*; Schiavello, M., Ed.; Kluwer Academic: New York, 1988; pp 469-497.

(6) (a) Xu, Z. Q.; Tongbao, X. *Huaxue Tongbao* 1989, 10, 26. (b) Fox, M. A.; Chen, C.-C. *Tetrahedron Lett.* 1983, 24, 547. (c) Ohtani, B.; Osaki, H.; Nishimoto, S.; Kagiya, T. *Chemistry Lett.* 1985, 1075.

\* Author to whom correspondence should be addressed.